

Toward *Ab initio* Simulation of Operando Raman Spectroscopy: Application to Sulfur/Carbon Copolymer Cathodes in Li-S Batteries

Rana Kiani,[†] Huiying Sheng,^{‡,¶} Timo Held,[†] Oliver Löhmann,[‡] Sebastian Risse,[‡]
Daniel Sebastiani,[†] and Pouya Partovi-Azar^{*,†}

[†]*Institute of Chemistry, Martin Luther University Halle-Wittenberg, Von-Danckelmann-Platz 4, 06120 Halle (Saale), Germany*

[‡]*Department for Electrochemical Energy Storage, Helmholtz-Zentrum Berlin für Materialien und Energie, Hahn-Meitner-Platz 1, Berlin, Germany*

[¶]*Department of Chemistry, Humboldt Universität zu Berlin, Brook-Taylor-Str. 2, 12489, Germany*

E-mail: pouya.partovi-azar@chemie.uni-halle.de

Abstract

Sulfur/carbon copolymers have emerged as a promising alternative for conventional crystalline sulfur cathodes for lithium-sulfur batteries. Among these, sulfur-*n*-1,3-diisopropenylbenzene (S/DIB) copolymers, which present a network of DIB molecules interconnected via sulfur chains, have particularly shown a good performance and, therefore, have been under intensive experimental and theoretical investigations. However, their structural complexity and flexibility have hindered a clear understanding of their structural evolution during redox reactions at an atomistic level. Here, by performing state-of-the-art finite-temperature *ab initio* Raman spectroscopy simulations, we investigate the spectral fingerprints of S/DIB copolymers during consecutive reactions with

lithium. We discuss in detail Raman spectral changes in particular frequency ranges which are common in S/DIB copolymers having short sulfur chains and those consisting of longer ones. We also highlight those distinctive spectroscopic fingerprints specific to local S/DIB structures containing only short or long sulfur chains. This distinction could serve to help distinguish between them experimentally. Our theoretically predicted results are in a good agreement with experimental Raman measurements on coin cells at different discharge stages. This work represents, for the first time, an attempt to compute *operando* Raman spectra using quantum-chemical calculations and provides a guideline for Raman spectral changes of arbitrary electrodes during the discharge.

Introduction

The remarkable theoretical specific capacity of elemental sulfur ($\simeq 1675$ mA h/g), its eco-friendly nature, and its abundance make lithium-sulfur (Li-S) batteries an attractive alternative to current lithium-ion batteries.^{1,2} Nevertheless, their cycle life has so far been limited due to certain drawbacks. A notable challenge is the formation of long-chain, soluble lithium polysulfides during the discharge and their shuttling through the conventional electrolytes,^{3,4} which leads to a depletion of the active material and formation of an insulating layer around the anode. All these processes result in an irreversible capacity fade in Li-S batteries.^{5,6} To tackle these issues, numerous studies have focused on structural optimization of sulfur cathodes including utilization of sulfur/carbon copolymers. In order to synthesize S/C copolymers, many researchers have employed the inverse vulcanization reaction as a facile synthesis method which provides a straightforward way for controlling sulfur content. Among others, sulfur-*n*-1,3-diisopropenylbenzene (S/DIB) copolymer has shown a promising performance as an active cathode material for Li-S batteries.^{7,8}

Structural characterization of S/DIB copolymers has been the subject of several studies so far.^{6,9-11} For example, similar to other S/C copolymers involving sulfur chains,¹²⁻¹⁸

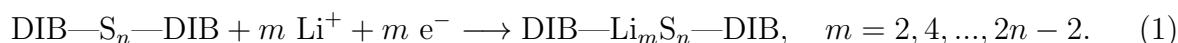
thermodynamically preferred S/DIB structures consist of short S_n chains, $n \simeq 4$.¹⁰ The shorter sulfur chains are expected to result in a hindrance in the formation of higher-order Li-polysulfides and consequently a stable cycling of 1500 cycles has been reported.¹⁹ Despite qualitative descriptions of the discharge mechanism of S/DIB copolymer cathodes,^{6,19} an atomistic view on their structural evolution during the lithiation reactions is still lacking. Such an insight can lead to morphology optimization of sulfur/carbon copolymers toward more efficient cathodes.

In this study, we aim to address the structural evolution of S/DIB copolymers during discharge by performing finite-temperature Raman spectroscopy simulations, combining quantum-chemical calculations with *ab initio* molecular dynamics simulations on model S/DIB systems. Here, we study the lithiation reactions of DIB- S_n -DIB with two different sulfur chain lengths, namely $n = 4$ and 8, and focus on Raman spectroscopic fingerprints of the final structures at different stages of discharge. The huge computational effort of such an investigation is substantially reduced by our efficient Wannier polarizability method for the estimation of the dynamics of polarizability tensors during *ab initio* molecular dynamics simulations,²⁰⁻²³ fully bypassing the time-consuming linear response calculations. We demonstrate common spectroscopic trends occurring during discharge of Li-S batteries based on S/DIB copolymer cathodes involving both short and long sulfur chains. Moreover, we predict spectroscopic fingerprints during the discharge specific to the copolymers having either short or long sulfur chains only. Our theoretical predictions are validated against Raman spectroscopy measurements on coin cells at different discharge states. These findings will contribute to the advancement of material analysis using *operando* measurements and thereby can lead to enhanced performance of Li-S batteries.

Methodology

Computational details

We consider DIB–S_{*n*}–DIB as target molecules in vacuum as a local structure of poly(sulfur-*n*-1,3-diisopropenylbenzene), where *n* = 4 and 8, representing copolymers consisting of short and long sulfur chains, respectively. In S/DIB copolymers, a sulfur chain connects to two DIB molecules. The terminal sulfur atoms forming C–S bonds are usually referred to as organic sulfur atoms. The C–S bonds remain stable during reactions with lithium,⁶ resulting in lithium-saturated chains where the number of lithium atoms reacting with the sulfur chain is twice the number of sulfur atoms minus two. Therefore, consecutive lithiation reactions of S/DIB copolymers are described by



In our computations, we treat the Li⁺ and e[−] pair as a single lithium atom. The initial structures are prepared by adding the Li atom along the S chain at distinct positions. These structures then go through atomic coordinate optimizations. In total, about 360 initial structures and optimizations have been carried out. At each lithiation state, the lowest-energy product structure is considered as a candidate for the actual lithiation product. As indicated in Eq. (1), we continue with sequential lithiation reactions until the saturation of the sulfur chain with lithium atoms is achieved. For simplicity, we specifically consider even numbers of lithium atoms in each reaction.

All quantum-chemical atomistic coordinate optimizations are performed at density-functional theory (DFT) level using the CP2K/QUICKSTEP software package²⁴ in conjunction with a DZVP-MOLOPT basis set,²⁵ as well as Perdew-Burke-Ernzerhof (PBE)²⁶ exchange-correlation energy functional and Geodecker Teter-Hutter (GTH) pseudopotentials.^{27,28} The semi-empirical DFT-D3²⁹ method is used to correct for the long-range dispersion

interactions. All calculations in this work are performed in vacuum.

After identifying the minimum-energy structure at each lithiation step, we study its structural stability by carrying out a 20 ps DFT-based *ab initio* molecular dynamics (AIMD) simulation in the canonical ensemble (NVT) at an elevated temperature of 500 K. In rare cases where an unexplored structure is formed at the elevated temperature, new geometry optimization is performed and the energy is compared to the previously found product structure at the corresponding lithiation step. In a following step, another round of AIMD simulations is performed on the structurally stable products for 20 ps in the NVT ensemble to achieve equilibrium at 300 K. This is followed by 20 ps of AIMD simulations in the micro-canonical ensemble (NVE) to sample the polarizabilities needed for the simulation of Raman spectra. A time step of 1 fs is used in the AIMD simulations, while the polarizabilities are sampled every 5 fs. The AIMD simulations are also performed using the CP2K software with the same simulation setup as mentioned earlier.

The Raman spectroscopy simulations are performed using the efficient Wannier polarizability method.^{20–23} This method allows for a very efficient estimation of the dynamics of the polarizability, which can be about 1000 times faster compared to the conventional approaches, for example those based on linear response theory.²³ Such an efficiency enables us to perform *ab initio* simulations of *operando* Raman spectroscopy.

The interaction energies are corrected for the basis set superposition error based on the counterpoise correction of Boys and Bernardi.³⁰

Materials and synthesis

All reagents, namely sulfur ($\geq 99.5\%$, Sigma-Aldrich), 1,3-diisopropenylbenzene (DIB, 97%, TCI), sodium carboxymethyl cellulose (CMC, MW 250,000, Sigma-Aldrich), polyacrylic acid (PAA, MW 450,000, Sigma-Aldrich), electrolyte (purchased from E-lyte) consisting of lithium bis(trifluoromethane)sulfonimide and 2 wt% lithium nitrate in a 1:1 *v/v* mixture of 1,3-dioxolane and 1,2-dimethoxy ethane, metallic lithium chips (99.95%, China Energy

Lithium), polypropylene separator (Celgard-2700), and carbon black (super p, Macklin) are used directly. SDIB10 was synthesized using the previously reported method.^{6,9,11,31} 10 wt% sulfur is added into a glass vial equipped with a magnetic stir bar and heated to 130 °C in a thermostated oil bath. DIB is added to the fully molten sulfur using a syringe and stirred for 10 minutes to achieve a homogeneous mixture. The resulting mixture is further heated to 185 °C for 8-10 minutes, which results in vitrification of the mixture. The product is then cooled down to room temperature. The obtained product is mixed with carbon black and binder mixture of CMC/PAA (1/1 *w/w*) in a mass ratio of 75:20:5 in water. The slurry is then ball milled and blade cast onto carbon coated aluminum foil. The areal mass loading of sulfur inside the electrode is around 3 mg/cm². After getting completely dried, the prepared electrode is cut into disks with 12 mm diameters to be used as cathode in a coin cell.

Instrumentation and measurements

The prepared cathodes are assembled into CR2032 coin cells with electrolyte, a polypropylene separator, and a lithium foil anode in an argon filled glove box. Cells are tested in a VMP3 potentiostats from 0.8-3 V at 0.1 C for 4 cycles. A renishaw QONTOR instrument with a 532 nm laser is employed for the *ex-situ* Raman spectroscopy in the range from 0-4000 cm⁻¹ with a resampling interval of 1 cm⁻¹. Cycled cathodes at 0%, 66%, and 100% depth of discharge and a cathode without cycling are measured.

Result and discussion

During structure optimizations and AIMD simulations at 500 K and 300 K, we do not observe any C-S bond breaking, irrespective of the sulfur chain length and the depth of discharge. However, we see a gradual breaking of S-S bonds in the course of discharge. This implies that the organic sulfur atoms play an important role in keeping the emerging lithium-sulfur structures connected to the organic groups via C-S bonds. This has also been argued earlier

to be one of the factors contributing to the good electrochemical performance of S/DIB copolymers by anchoring the emerging lithium-sulfur structures to the organic groups.⁶ In fact, here we find the interaction energies between the lithium-sulfur structures and the organic groups (DIB molecules together with organic sulfur atoms) at 100% depth of discharge to be about 1.4 times as high as a typical C–S covalent bond ($E_{C-S} \simeq 7.2$ eV)³² both in DIB–Li₆S₄–DIB and DIB–Li₁₄S₈–DIB.

Calculated room-temperature *ab initio* Raman spectra of DIB–S₄–DIB and DIB–S₈–DIB molecules at different stages of discharge are shown in Fig. 1 and Fig. 2, respectively. The corresponding lithiated structures are also shown in the insets. Decomposing the total Raman spectra into local contributions,^{21–23} we find that among all Raman activities spanning 0–3300 cm⁻¹ range, the signals in 0–1200 cm⁻¹ predominantly arise from the emerging lithium-sulfur structure between two DIB molecules [Fig. 1(a), panel (IV) and Fig. 2(a), panel (VIII)]. The observed signals in the higher frequency range (1200–3300 cm⁻¹) mostly correspond to vibrations of the DIB molecules (see Fig. S1 in the Supplementary Information). Here, we particularly focus on the activities arising from lithium-sulfur structures.

S/DIB copolymers with short sulfur chains

The Raman spectra obtained for the DIB–S₄–DIB structure [Fig. 1(a), panel (I)] agrees well with earlier investigations.¹¹ The activities observed at around 100 cm⁻¹ and 350 cm⁻¹ in Fig. 1(a), panel(I), are attributed to S₄ chain deformations in the DIB–S₄–DIB structure. However, as seen in Fig. 1(a), these activities become unnoticeable upon reaction with lithium due to the breaking of S–S bonds along the chain. Based on our observation, as the copolymer is discharged to around 33% [Fig. 1(a), panel (II)], the S₄ chain splits at the mid-bond, resulting in the formation of two shorter S₂ chains. As the lithiation continues, another sulfur bond is broken [Fig. 1(a), panel (III)]. The same pattern is observed until the final lithiation stage, where no S–S covalent bond is present anymore [Fig. 1(a), panel (IV)]. Additionally, the lithiation reactions appear to be reversible. The reversibility of the

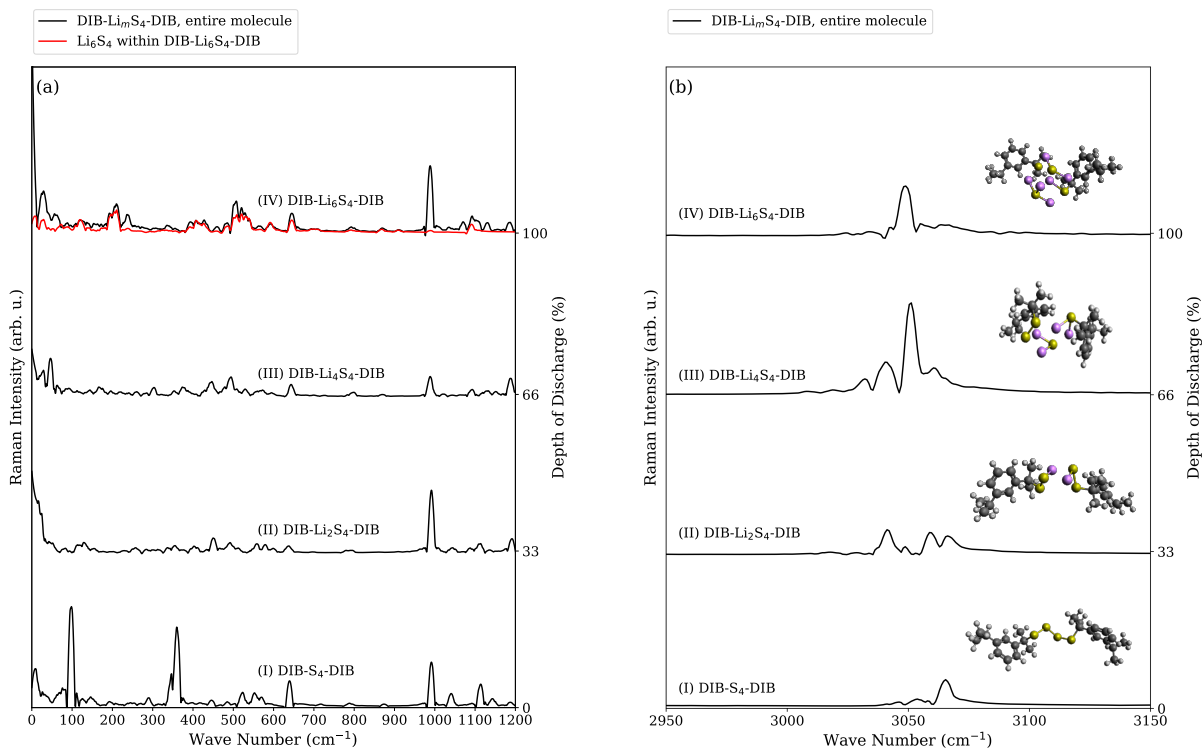


Figure 1: Computed Raman spectra for (I) DIB-S₄-DIB, (II) DIB-Li₂S₄-DIB, (III) DIB-Li₄S₄-DIB, and (IV) DIB-Li₆S₄-DIB molecules in vacuum. (a) Spectra in the range of 0–1200 cm⁻¹ and (b) Spectra in the range of 2950–3150 cm⁻¹. The black curves represent the computed Raman spectra of the entire DIB-Li_mS₄-DIB molecule, while the red curve represents the partial Raman spectra of Li₆S₄ within the DIB-Li₆S₄-DIB molecule. Note that the intensities in (b) are multiplied by ten.

reactions is particularly checked by removing two lithium atoms from the optimized DIB–Li₄S₄–DIB structure [Fig. 1(a), panel (III)] followed by an atomic coordinate optimization on the resulting structure. We observe a restoration of a broken S–S bond leading to a DIB–Li₂S₄–DIB structure, similar to the one shown in Fig. 1(a), panel (II).

At 100% depth of discharge, where the system contains the highest possible number of lithium atoms, a notable Raman activity is observed around 200 cm⁻¹, as shown in Fig. 1(a), panel (IV). This activity can be attributed to the lithium-sulfur structure.³³

Moreover, in agreement with previous studies²¹ where the Raman activities in the range of 350–500 cm⁻¹ have predominantly been attributed to lithium-sulfur structure, our results reveal a gradual increase in Raman activities within the 400–500 cm⁻¹ range as more lithium atoms react with sulfur [Fig. 1(a)]. In the range of 480–580 cm⁻¹, specifically at 520 cm⁻¹, a broad Raman activity is observed as the depth of discharge reaches 100%, which should also arise from the formation of lithium-sulfur structure.³³

Based on partial Raman analysis, the activity at ~575 cm⁻¹ can be assigned to the C–S bond stretching [see Fig. S6 in the Supplementary Information].¹¹ In agreement with our observation, it has been shown before¹⁹ that this peak gets slightly blueshifted during the discharge.

The activity in about 650, 710, 790, 870, and 900 cm⁻¹ Raman shifts can be due to collective Raman-active vibrations of lithium-sulfur structures and the DIB groups (see Fig. S6 in Supplementary Information for partial spectra). These vibrations are observed in all lithiated samples of DIB–S₄–DIB and DIB–S₈–DIB. This also holds for the activities seen around 1100 cm⁻¹ (see Fig. 1(a), panel (IV) and the Supplementary Information).

The vibrational mode around 1000 cm⁻¹ is a strong indicator of a benzene ring breathing vibration in all systems. Here, we observe that the intensity of this mode fluctuates non-monotonically with the depth of discharge. As will be discussed later, the intensity of this band could be heavily affected by the presence of binder material and/or carbon black.

Furthermore, we observe that the formation of lithium-sulfur structures could have a

far-reaching effect. For example, as shown in Fig. 1(b), we see that the frequency range attributed to the C–H stretching vibrations becomes broader as a function of the depth of discharge. For clarity, the intensities are scaled up ten times compared to Fig. 1(a). A redshift is seen in the frequency of the dominant peak at $\sim 3065\text{ cm}^{-1}$ [Fig. 1(b), panel (I)] towards $\sim 3048\text{ cm}^{-1}$ [Fig. 1(b), panel (IV)] in the course of discharge. The decomposition of the spectra reveals that the observed redshift corresponds to the weakening of the C–H bonds proximal to the lithiation center (see Fig. S2 in the Supplementary Information).

S/DIB copolymers with long sulfur chains

The calculated Raman spectra of a DIB–Li_mS₈–DIB molecule at different stages of discharge are presented in Fig. 2(a), panels (I)–(VIII). The Raman spectrum of DIB–S₈–DIB structure [Fig. 2(a), panel (I)] agrees well with our previous investigations on S/DIB copolymers with long sulfur chains.¹¹ In the range of 100–180 cm^{-1} , two prominent peaks are observed. In our previous study, these activities in copolymers with longer sulfur chains have been attributed to sulfur chain deformation and S–S–S bending, and they gradually decline with increasing weight percentage of DIB.

At a discharge state of approximately 14% [Fig. 2(a), panel (II)], we observe a structure with one broken S–S bond, resulting in two shorter chains, namely S₃ and S₅. As lithiation continues, an additional sulfur bond is broken [Fig. 2(a), panel (III)]. Similar to the case of DIB–S₄–DIB, this pattern continues during further lithiations up to the final stage of discharge, where there is no S–S covalent bond remaining in DIB–Li₁₄S₈–DIB [Fig. 2(a), panel (VIII)]. Here, we also observe that S–S bond breaking can be reversible as well.

Upon splitting of the S₈ chain in DIB–S₈–DIB at early stages of discharge [Fig. 2(a), panel (II)], we observe rather intensive Raman activities in the range of 100–250 cm^{-1} , resembling those previously observed in free (isolated) S₄ and S₈ chains.¹¹ This shows that the S/DIB copolymer cathode should involve quasi-free S chains at low depths of discharge. Here, these activities are attributed to S–S–S bending within the S₅ unit of DIB–Li₂S₈–DIB (see Fig. S3

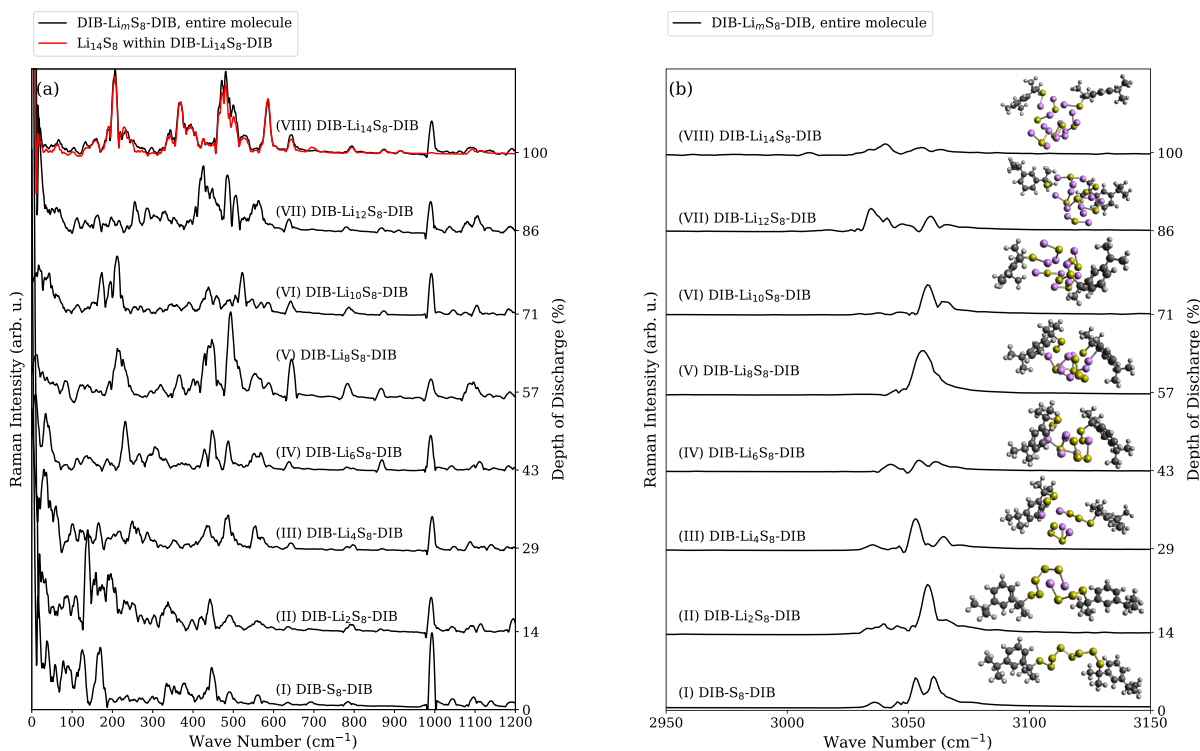


Figure 2: Computed Raman spectra for (I) DIB-S₈-DIB, (II) DIB-Li₂S₈-DIB, (III) DIB-Li₄S₈-DIB, (IV) DIB-Li₆S₈-DIB, (V) DIB-Li₈S₈-DIB, (VI) DIB-Li₁₀S₈-DIB, (VII) DIB-Li₁₂S₈-DIB, and (VIII) DIB-Li₁₄S₈-DIB molecules in vacuum. (a) Spectra in the range of 0–1200 cm⁻¹ and (b) Spectra in the range of 2950–3150 cm⁻¹. The black curves represent the computed Raman spectra of the entire DIB-Li_mS₈-DIB molecule, while the red curve represents the partial Raman spectra of Li₁₄S₈ within DIB-Li₁₄S₈-DIB molecule.

and S4 in Supplementary Information for further details).

As the system gets further lithiated, a significant Raman activity is observed at around 200 cm^{-1} [Fig. 2(a), panels (II)-(VIII)]. Similar to the case of DIB-Li_mS₄-DIB [Fig. 1(a)], this activity can generally be assigned to the emerging lithium-sulfur structure.

Similarly, Raman activities in the $320\text{-}400$ and $420\text{-}600\text{ cm}^{-1}$ ranges arise from the lithium-sulfur structures. These activities become more noticeable with increasing number of lithium atoms. At 100% depth of discharge [Fig. 2(a), panel (VIII)], the dominant Raman activity in $320\text{-}400\text{ cm}^{-1}$ range coincides with the characteristic Raman activity of Li₂S solid.³⁴

The Raman activity around 450 cm^{-1} predominantly originates from S-S stretching vibration in longer sulfur chains. This activity is a key factor in distinguishing between long and short sulfur chains, as previously discussed.¹¹ The activity at $\sim 450\text{ cm}^{-1}$ is found to be absent at 100% depth of discharge as there is no S-S covalent bond present in the DIB-Li₁₄S₄-DIB molecule anymore. Instead, a broad activity emerges at 100% depth of discharge at $470\text{-}550\text{ cm}^{-1}$ which seems to come almost entirely from the formed lithium-sulfur structure [see the red curve in Fig. 2(a), panel (VIII)]. However, our analysis based on partial Raman spectrum of the S₈ chain within DIB-S₈-DIB shows that the activity at $\sim 480\text{ cm}^{-1}$ should partially arise from the DIB molecules as well. It is worth noting that this activity arising from the organic molecules should be present at all stages of discharge.

Similar to the case of DIB-S₄-DIB, the activity at $\sim 575\text{ cm}^{-1}$ can be attributed to the C-S bond stretching [see Fig. S6 in the Supplementary Information].¹¹ In qualitative agreement with previous studies,¹⁹ this peak undergoes a blueshift from $\sim 575\text{ cm}^{-1}$ to $\sim 585\text{ cm}^{-1}$ during discharge.

The activity in the $600\text{-}900\text{ cm}^{-1}$ range can also be attributed to collective Raman-active vibrations of sulfur (either lithiated or otherwise) and the organic groups (see also Fig. S6 in Supplementary Information for partial spectra). As in the case of DIB-S₄-DIB, the activities seen around 1100 cm^{-1} should also arise from similar coupled Li-S/DIB vibrations (see the Supplementary Information).

We also observe a similar behavior in the C–H stretching frequency range as in DIB–S₄–DIB. As shown in Fig. 2(b), the frequency range associated with C–H stretching bandwidth broadens with increasing depth of discharge. However, in the case of DIB–S₈–DIB, no

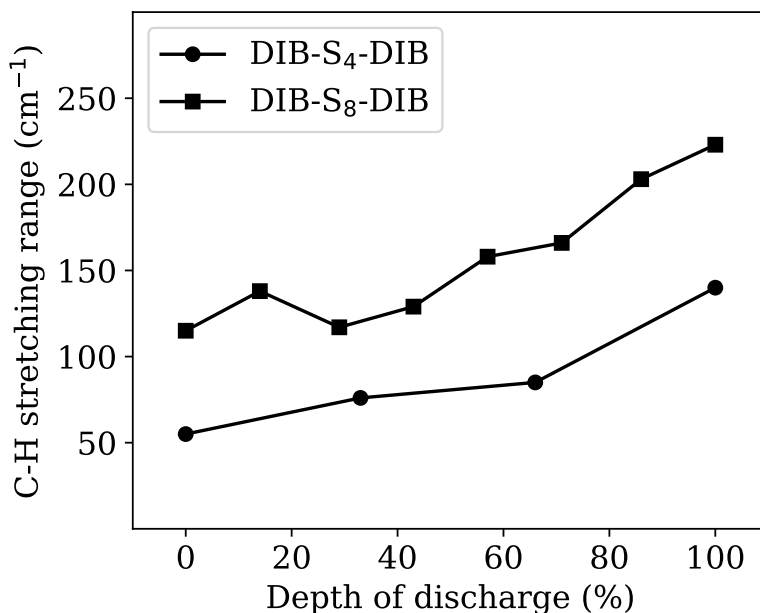


Figure 3: C–H stretching bandwidth as a function of depth of discharge for DIB–S₄–DIB (circles) and DIB–S₈–DIB (squares).

meaningful frequency shift is observed. Fig. 3 illustrates how the C–H stretching bandwidth increases during the discharge process for both sulfur chain lengths (S₄ and S₈). This broadening indicates that the introduction of lithium into the system and hence its interaction with sulfur atoms affects C–H bonds vibrations, resulting in nonidentical oscillators (see Fig. S2 in the Supplementary Information for partial Raman analysis).

Comparing panel (IV) in Fig. 1(a) with panel (VIII) in Fig. 2(a), we observe that S/DIB copolymers containing short chains and those having long ones show similar Raman features at 100% depth of discharge. The main difference is that the bands are broader in the case of DIB–S₈–DIB. This is due to the fact that in lithiated DIB–S₈–DIB structure, the number of nonidentical oscillators with Raman activities at certain frequency ranges are higher than

that in the DIB-S₄-DIB system at the same frequency ranges. However, the Raman activity at $\sim 450\text{ cm}^{-1}$ corresponding to the S-S stretching mode could again serve as a fingerprint for distinguishing between local copolymer structures consisting of short and long sulfur chains. Although the corresponding band shows an insignificant intensity at 0% depth of discharge in DIB-S₄-DIB [Fig. 1(a), panel (I)], it exhibits an intensive band in DIB-S₈-DIB from 0% up to 86% depth of discharge [Fig. 2(a), panels (I)-(VII)]. At 100% depth of discharge, where no S-S covalent bond is present, the intensity of this band becomes negligibly small in both DIB-Li₆S₄-DIB and DIB-Li₁₄S₈-DIB structures. In addition to this band, the Raman activities at $\sim 200\text{ cm}^{-1}$ during discharge can also be used to distinguish between short and long sulfur chains. While the band at $\sim 200\text{ cm}^{-1}$ only appears at fully discharged DIB-S₄-DIB [Fig. 1(a)], our results show a rather intensive activity in 200-250 cm^{-1} range at 14% to 100% depth of discharge of DIB-S₈-DIB [Fig. 2(a), panels (II)-(VI)].

Comparison with Raman measurements

Figure 4 shows the *ex-situ* measured Raman spectra of the synthesized SDIB10 sample which corresponds to an average sulfur chain length of 22 sulfur atoms. All the intensities are normalized with respect to the carbon D band at $\sim 1350\text{ cm}^{-1}$. The spectra are at different depths of discharge, namely %0 (black), %66 (red), and 100% (blue). Despite differing sulfur chain lengths, these spectra can be qualitatively compared with those presented in Fig. 2(a) for DIB-S₈-DIB. It is worth noting that apart from activities coming from the S/DIB copolymer, those from the electrolyte, carbon black, and binder material are also present in the experimental spectra. Therefore, here the comparison between theory and experiment can only be qualitative.

Although the relative intensities in the spectrum corresponding to 0% depth of discharge in Fig. 4 (black curve) do not fully match with those in panel (I) of Fig. 2(a), the peak positions agree well. As discussed earlier, the activity at around 200 cm^{-1} in Fig. 4 should come from sulfur chain deformation at early stages of discharge. The collective vibrations in the lithium-

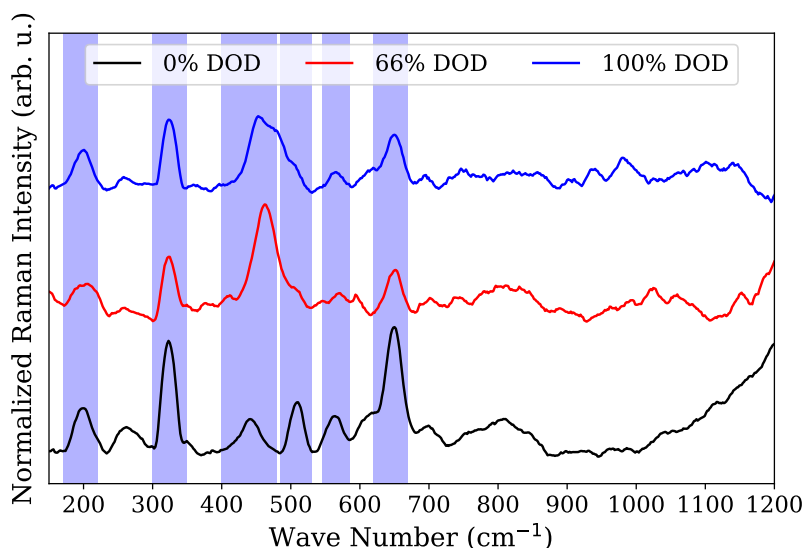


Figure 4: Experimental Raman measurement on SDIB10. DOD stands for depth of discharge.

sulfur structure toward the end of discharge also have an activity around the same frequency. The activity in $300\text{-}400\text{ cm}^{-1}$ in the black curve in Fig. 4 (0% depth of discharge) can also be attributed to sulfur chain deformation, as has been revealed in our previous study.¹¹ This activity, similar to the one at $\sim 200\text{ cm}^{-1}$ also arises from lithium-sulfur vibrations at higher depths of discharge [Fig. 2(a), panel (VIII)]. As discussed earlier, the activity at $\sim 450\text{ cm}^{-1}$ can be assigned to S-S stretching, the one at $\sim 500\text{ cm}^{-1}$ to DIB vibrations, $\sim 560\text{ cm}^{-1}$ to C-S stretching, and finally those at $\sim 650\text{ cm}^{-1}$ to coupled (lithium-)sulfur/DIB vibrations. These assignments can be further justified based on the fact that, for example, the peak at $\sim 450\text{ cm}^{-1}$ is found to become unnoticeable at 100% depth of discharge (blue curve), while the ones at $\sim 500\text{ cm}^{-1}$, $\sim 560\text{ cm}^{-1}$, and $\sim 650\text{ cm}^{-1}$ are found at all stages of discharge. A clear broad activity is observed in Fig. 4 in $450\text{-}500\text{ cm}^{-1}$ range. Our calculations show that this broad activity arises mostly from the emerging lithium-sulfur structure and is found to occur in a comparable frequency range, namely $470\text{-}550\text{ cm}^{-1}$.

Conclusions

In summary, we have investigated the spectral evolution of sulfur/1,3-diisopropenylbenzene (S/DIB) copolymers as a function of depth of discharge by performing *ab initio* finite-temperature Raman spectroscopy simulations. The focus has been set on the spectroscopic fingerprints arising from local S/DIB structures containing low and high sulfur content, corresponding to short and long sulfur chains, respectively. This study, to the best of our knowledge, represents the first attempt toward quantum-chemical simulation of *operando* Raman spectroscopy based on *ab initio* molecular dynamics simulations. This has been made feasible by using the Wannier polarizability method to efficiently sample the polarizability dynamics.

Our current study dives deeper into understanding the complex discharge mechanisms of S/DIB copolymer cathodes. We have observed that S/DIB copolymers containing short and those consisting of long sulfur chains show similar Raman features at 100% depth of discharge. However, we have found frequency ranges in which short- and long-sulfur chain containing copolymers have distinctive Raman activities during the discharge. For example, the Raman activity at $\sim 450\text{ cm}^{-1}$ (S–S stretching) can serve as a fingerprint for distinguishing between local copolymer structures consisting of short and long sulfur chains. Although the corresponding band shows an insignificant intensity at early to mid stages of discharge in S/DIB polymers with short sulfur chains, it shows an intensive band in those containing long sulfur chains from 0% up to 86% depth of discharge. At 100% depth of discharge, where no S–S covalent bond is present, the intensity of this band can become negligibly small in all S/DIB samples. In addition to this, the Raman activities at $\sim 200\text{ cm}^{-1}$ during the discharge can also be used to distinguish between short and long sulfur chains. The band at $\sim 200\text{ cm}^{-1}$ only appears at fully discharged S/DIB copolymers with short sulfur chains. However, we have found a rather intensive activity in $200\text{--}250\text{ cm}^{-1}$ range at 14% to 100% depth of discharge of those copolymers consisting of long sulfur chains. These theoretical predictions have been validated against *ex-situ* Raman measurements on S/DIB cathodes at

different stages of discharge and provide practical insights into designing and characterizing sulfur/carbon copolymers cathode materials.

Acknowledgement

The authors gratefully acknowledge DFG funding via projects PA3141/3 (Project number 420536636), PA3141/5 (Project number 446879138), and SPP 2248 “Polymer-based Batteries”. Additionally, H.S. kindly acknowledges the financial support from the China Scholarship Council (No. 202308080034). The computations have been mostly performed on a Bull Cluster at the Center for Information Services and High Performance Computing (ZIH) at TU Dresden via the project ‘p_oligothiophenes’.

Supporting Information Available

Supporting Information is available on Raman peak assignments based on partial Raman analysis, and lithiation reaction energies.

References

- (1) Winter, M.; Brodd, R. J. What are batteries, fuel cells, and supercapacitors? *Chemical reviews* **2004**, *104*, 4245–4270.
- (2) Bruce, P. G. Energy storage beyond the horizon: Rechargeable lithium batteries. *Solid State Ionics* **2008**, *179*, 752–760.
- (3) Liang, X.; Hart, C.; Pang, Q.; Garsuch, A.; Weiss, T.; Nazar, L. F. A highly efficient polysulfide mediator for lithium–sulfur batteries. *Nature communications* **2015**, *6*, 5682.
- (4) Seh, Z. W.; Sun, Y.; Zhang, Q.; Cui, Y. Designing high-energy lithium–sulfur batteries. *Chemical society reviews* **2016**, *45*, 5605–5634.

- (5) Simmonds, A. G.; Griebel, J. J.; Park, J.; Kim, K. R.; Chung, W. J.; Oleshko, V. P.; Kim, J.; Kim, E. T.; Glass, R. S.; Soles, C. L., et al. Inverse vulcanization of elemental sulfur to prepare polymeric electrode materials for Li–S batteries. *ACS Macro Letters* **2014**, *3*, 229–232.
- (6) Hoefling, A.; Nguyen, D. T.; Partovi-Azar, P.; Sebastiani, D.; Theato, P.; Song, S.-W.; Lee, Y. J. Mechanism for the Stable Performance of Sulfur-Copolymer Cathode in Lithium–Sulfur Battery Studied by Solid-State NMR Spectroscopy. *Chemistry of Materials* **2018**, *30*, 2915–2923.
- (7) Evers, S.; Nazar, L. F. New approaches for high energy density lithium–sulfur battery cathodes. *Accounts of chemical research* **2013**, *46*, 1135–1143.
- (8) Ji, X.; Nazar, L. F. Advances in Li–S batteries. *Journal of Materials Chemistry* **2010**, *20*, 9821–9826.
- (9) Chung, W. J.; Griebel, J. J.; Kim, E. T.; Yoon, H.; Simmonds, A. G.; Ji, H. J.; Dirlam, P. T.; Glass, R. S.; Wie, J. J.; Nguyen, N. A., et al. The use of elemental sulfur as an alternative feedstock for polymeric materials. *Nature chemistry* **2013**, *5*, 518–524.
- (10) Kiani, R.; Sebastiani, D.; Partovi-Azar, P. On the Structure of Sulfur/1, 3-Diisopropenylbenzene Co-Polymer Cathodes for Li-S Batteries: Insights from Density-Functional Theory Calculations. *ChemPhysChem* **2022**, *23*, e202100519.
- (11) Kiani, R.; Steimecke, M.; Alqaisi, M.; Bron, M.; Sebastiani, D.; Partovi-Azar, P. Characterization of sulfur/carbon copolymer cathodes for Li-S batteries: a combined experimental and ab initio Raman spectroscopy study. **2023**,
- (12) Schütze, Y.; de Oliveira Silva, R.; Ning, J.; Rappich, J.; Lu, Y.; Ruiz, V. G.; Bande, A.; Dzubiella, J. Combined first-principles statistical mechanics approach to sulfur structure in organic cathode hosts for polymer based lithium–sulfur (Li–S) batteries. *Physical Chemistry Chemical Physics* **2021**, *23*, 26709–26720.

- (13) Schütze, Y.; Gayen, D.; Palczynski, K.; de Oliveira Silva, R.; Lu, Y.; Tovar, M.; Partovi-Azar, P.; Bande, A.; Dzubiella, J. How Regiochemistry Influences Aggregation Behavior and Charge Transport in Conjugated Organosulfur Polymer Cathodes for Lithium–Sulfur Batteries. *ACS Nano* **2023**, DOI: 10.1021/acsnano.3c01523.
- (14) Zou, R.; Liu, W.; Ran, F. Sulfur-containing polymer cathode materials: From energy storage mechanism to energy density. *InfoMat* **2022**, e12319.
- (15) Park, S.; Kim, S.-J.; Sung, Y.-E.; Char, K.; Son, J. G. Short-chain polyselenosulfide copolymers as cathode materials for lithium–sulfur batteries. *ACS applied materials & interfaces* **2019**, *11*, 45785–45795.
- (16) Partovi-Azar, P.; Jand, S. P.; Kaghazchi, P. Electronic, magnetic, and transport properties of polyacrylonitrile-based carbon nanofibers of various widths: density-functional theory calculations. *Physical Review Applied* **2018**, *9*, 014012.
- (17) Partovi-Azar, P. Sulfur/Polyacrylonitrile-Based N-Terminated Graphene Nanoribbon Cathodes for Li-S Batteries. *Physical Review Applied* **2022**, *18*, 044072.
- (18) Huang, C.-J.; Cheng, J.-H.; Su, W.-N.; Partovi-Azar, P.; Kuo, L.-Y.; Tsai, M.-C.; Lin, M.-H.; Jand, S. P.; Chan, T.-S.; Wu, N.-L., et al. Origin of shuttle-free sulfurized polyacrylonitrile in lithium-sulfur batteries. *Journal of Power Sources* **2021**, *492*, 229508.
- (19) Rafie, A.; Pereira, R.; Shamsabadi, A. A.; Kalra, V. In Operando FTIR Study on the Effect of Sulfur Chain Length in Sulfur Copolymer-Based Li–S Batteries. *The Journal of Physical Chemistry C* **2022**, *126*, 12327–12338.
- (20) Partovi-Azar, P.; Kühne, T. D. Efficient “On-the-Fly” calculation of Raman Spectra from Ab-Initio molecular dynamics: Application to hydrophobic/hydrophilic solutes in bulk water. *Journal of Computational Chemistry* **2015**, *36*, 2188–2192.

- (21) Partovi-Azar, P.; Kühne, T. D.; Kaghazchi, P. Evidence for the existence of Li_2S_2 clusters in lithium–sulfur batteries: ab initio Raman spectroscopy simulation. *Physical Chemistry Chemical Physics* **2015**, *17*, 22009–22014.
- (22) Partovi-Azar, P.; Kühne, T. D. Full Assignment of Ab-Initio Raman Spectra at Finite Temperatures Using Wannier Polarizabilities: Application to Cyclohexane Molecule in Gas Phase. *Micromachines* **2021**, *12*, 1212.
- (23) Partovi-Azar, P. Efficient method for estimating the dynamics of the full polarizability tensor during ab initio molecular dynamics simulations. *Physical Review B* **2023**, *108*, 235157.
- (24) Kühne, T. D.; Iannuzzi, M.; Del Ben, M.; Rybkin, V. V.; Seewald, P.; Stein, F.; Laino, T.; Khaliullin, R. Z.; Schütt, O.; Schiffmann, F., et al. CP2K: An electronic structure and molecular dynamics software package-Quickstep: Efficient and accurate electronic structure calculations. *The Journal of Chemical Physics* **2020**, *152*, 194103.
- (25) VandeVondele, J.; Hutter, J. Gaussian basis sets for accurate calculations on molecular systems in gas and condensed phases. *The Journal of chemical physics* **2007**, *127*, 114105.
- (26) Perdew, J. P.; Burke, K.; Ernzerhof, M. Generalized gradient approximation made simple. *Physical review letters* **1996**, *77*, 3865.
- (27) Goedecker, S.; Teter, M.; Hutter, J. Separable dual-space Gaussian pseudopotentials. *Physical Review B* **1996**, *54*, 1703.
- (28) Krack, M. Pseudopotentials for H to Kr optimized for gradient-corrected exchange-correlation functionals. *Theoretical Chemistry Accounts* **2005**, *114*, 145–152.
- (29) Grimme, S.; Antony, J.; Ehrlich, S.; Krieg, H. A consistent and accurate ab initio

- parametrization of density functional dispersion correction (DFT-D) for the 94 elements H-Pu. *The Journal of chemical physics* **2010**, *132*, 154104.
- (30) Boys, S. F.; Bernardi, F. The calculation of small molecular interactions by the differences of separate total energies. Some procedures with reduced errors. *Molecular physics* **1970**, *19*, 553–566.
- (31) Berndt, A. J.; Hwang, J.; Islam, M. D.; Sihn, A.; Urbas, A. M.; Ku, Z.; Lee, S. J.; Czaplewski, D. A.; Dong, M.; Shao, Q., et al. Poly (sulfur-random-(1, 3-diisopropenylbenzene)) based mid-wavelength infrared polarizer: optical property experimental and theoretical analysis. *Polymer* **2019**, *176*, 118–126.
- (32) Brunton, L.; Hilal-Dandan, R.; Knollmann, B. McGraw-Hill Education: New York. NY, USA **2017**,
- (33) Lang, S.; Yu, S.-H.; Feng, X.; Krumov, M. R.; Abruña, H. D. Understanding the lithium–sulfur battery redox reactions via operando confocal Raman microscopy. *Nature communications* **2022**, *13*, 4811.
- (34) Lin, Z.; Liu, Z.; Dudney, N. J.; Liang, C. Lithium superionic sulfide cathode for all-solid lithium–sulfur batteries. *ACS nano* **2013**, *7*, 2829–2833.